

## <sup>1</sup>H HR-MAS NMR and S180 Cells: Metabolite Assignment and Evaluation of Pulse Sequence

Aline L. de Oliveira,<sup>a,b</sup> Bruno César B. Martinelli,<sup>b</sup> Luciano M. Lião,<sup>b</sup> Flávia C. Pereira,<sup>c</sup>  
Elisangela P. Silveira-Lacerda<sup>c</sup> and Glaucia B. Alcantara<sup>\*,d</sup>

<sup>a</sup>Instituto de Química, Universidade de Brasília, CP 04478, 70904-970 Brasília-DF, Brazil

<sup>b</sup>Laboratório de RMN, Instituto de Química, Universidade Federal de Goiás,  
CP 131, 74001-970 Goiânia-GO, Brazil

<sup>c</sup>Laboratório Genética Molecular e Citogenética, Instituto de Ciências Biológicas,  
Universidade Federal de Goiás, CP 131, 74001-970 Goiânia-GO, Brazil

<sup>d</sup>Instituto de Química, Universidade Federal de Mato Grosso do Sul,  
CP 549, 79070-900 Campo Grande-MS, Brazil

Ressonância magnética nuclear de <sup>1</sup>H de alta resolução com giro no ângulo mágico (HR-MAS NMR) é uma técnica empregada na avaliação de células e tecidos intactos. Entretanto, parâmetros bem estabelecidos de NMR são cruciais para a obtenção de resultados confiáveis. A fim de discutir as principais etapas envolvidas na otimização das análises de HR-MAS NMR, este artigo avaliou diferentes sequências de pulsos e parâmetros de NMR usando células de sarcoma 180 (S180). O completo assinalamento dos metabólitos de S180 é também apresentado para auxiliar estudos futuros.

High resolution magic angle spinning <sup>1</sup>H nuclear magnetic resonance spectroscopy (HR-MAS NMR) is a useful technique for evaluation of intact cells and tissues. However, optimal NMR parameters are crucial in obtaining reliable results. To identify the key steps for the optimization of HR-MAS NMR parameters, we assessed different pulse sequences and NMR parameters using sarcoma 180 (S180) cells. A complete assignment of the metabolites of S180 is given to assist future studies.

**Keywords:** HR-MAS NMR, sarcoma 180, S180, CPMG

### Introduction

Cancer is among the leading causes of death globally. It is well known that early diagnosis is crucial for effective treatment. The development of new techniques for detection of cancer prior to its progression has become an important challenge for the scientific community. High resolution magic angle spinning <sup>1</sup>H nuclear magnetic resonance spectroscopy (HR-MAS NMR) offers the potential to distinguish tumor types and to investigate tissues, detecting metabolic profiles and consequently cell biomarkers.<sup>1</sup> In recent years, studies of brain,<sup>2,3</sup> breast,<sup>4</sup> colorectal,<sup>5</sup> and lung tumors,<sup>6</sup> among others, have confirmed HR-MAS NMR as a promising technique in cancer diagnosis.

At the same time, with the arrival of the metabolomic era, many studies applying HR-MAS NMR have been undertaken to monitor metabolic changes in tumor cells. The assessment of changes in metabolic profile has been found especially useful in studying the efficacy and safety of new drugs or in monitoring disease progression for clinical purposes.<sup>7-11</sup> Additionally, the use of HR-MAS NMR has other advantages, such as providing qualitative, quantitative and structural information, and detecting a wide range of metabolites simultaneously in a single spectrum.

On the other hand, because of the great complexity of the cell matrix, several works have shown that minor variations of analyzed data make it important to discriminate differences in metabolism, demanding the application of statistical methods to obtain useful results.

\*e-mail: glaucia.alcantara@ufms.br

To obtain good results and highly reproducible spectra, it is necessary to optimize NMR experiments before applying refined data analysis. Sample preparation, temperature and choice of pulse sequences must be optimized. For this reason, it is very important that NMR acquisition parameters are optimized to avoid distortion of the data, such as distortions in phase and baseline caused by incomplete water suppression.<sup>12-14</sup>

In this context, to develop a robust methodology and to establish a procedure for diagnostic <sup>1</sup>H HR-MAS NMR, we assessed four pulse sequences. We also assessed the effects of variations in the acquisition parameters of CPMG (Carr-Purcell-Meiboom-Gill) pulse sequences. Studies employing NMR HR-MAS to evaluate cancer tissues frequently apply CPMG pulse sequences to suppress broad signals, which may overlap significant peaks of interest and make metabolomic analysis difficult.<sup>1</sup> To our knowledge, no published study has discussed the optimization of the  $\tau$  and  $n$  parameters of the CPMG pulse sequence.

All NMR data were obtained at room temperature (23 °C) using sarcoma 180 (S180) cells. S180 is a frequently studied murine tumor, an excellent model that is used especially for testing drug candidates with potential anticancer activity.<sup>15-17</sup> Thus, this study was also intended to assist future work through the full assignment of S180 metabolites.

## Materials and Methods

### Animal-handling procedure and sample preparation

Swiss mice aged 6-8 weeks and weighing 30-35 g were provided by the Central Animal Facility of UFG, and were maintained at the Laboratory of Experimental Oncology at the Department of General Biology, Institute of Biological Sciences I, at UFG, in ventilated racks EB275C model with 3-5 animals *per* mini insulator, under controlled temperature (22 ± 3 °C) and light-dark cycle of 12 h room conditions. The animals were maintained on standard diet with commercial feed and water *ad libitum*. All experimental procedures were approved by the Ethics Committee on Animal Use of UFG, under protocol number 039/12.

Sarcoma 180 (S180) cells (ascitic murine sarcoma) were purchased from the ATCC cell bank. The cell line was maintained in mice by intraperitoneal inoculation; transplantation was performed every ten days. After tumor stimulation, mice were sacrificed by cervical dislocation under sterile conditions. Then, S180 cells were aspirated removed from the intraperitoneal cavity with a syringe, transferred to a Falcon tube and centrifuged for 10 minutes at 1500 rpm at room temperature.

The supernatant was discarded and the pellet resuspended in 5 mL of RPMI 1640 medium supplemented with 10% fetal bovine serum (FBS), treated with penicillin and streptomycin, and centrifuged again. Aliquots of the pellets (40  $\mu$ L, equivalent to  $5 \times 10^5$  cells) were inserted in the HR-MAS rotor with 10  $\mu$ L of TMSP- $d_4$ /D<sub>2</sub>O (sodium-2,2,3,3- $d_4$ -3-trimethylsilylpropionate in deuterium oxide, 0.1%).

Fresh S180 samples were obtained from five different mice according to the above procedure for comparison among replicates. A control sample (RPMI 1640 medium supplemented with 10% FBS in TMSP- $d_4$ /D<sub>2</sub>O) was evaluated to detect contaminants.

### <sup>1</sup>H HR-MAS NMR spectra

All <sup>1</sup>H HR-MAS NMR measurements were carried out on a Bruker Avance III 500 instrument (operating at 500.13 MHz) equipped with a 4 mm HR-MAS probe and 50  $\mu$ L zirconium rotor. TMSP- $d_4$ /D<sub>2</sub>O was used for lock and field homogeneity adjustment. Spectra were collected at 5 kHz spin rate with temperature held constant at 23 °C.

Four different pulse sequences were tested. Two of these were common pulse sequences for water suppression using pre-saturation pulse (ZGPR) and composite pulse (ZGCPPR). A one-dimensional NOESY pulse sequence (NOESYPR1D) was also assessed (recycle delay-90- $t_1$ -90- $t_m$ -90-acquisition, with  $t_1$  delay 3  $\mu$ s and mixing time [ $t_m$ ] 100 ms). Finally, the CPMG spin-echo pulse sequence with pre-saturation (CPMGPR1D) was also evaluated. The CPMG pulse sequence is as follows: recycle delay – [–90°– ( $\tau$  – 180° –  $\tau$ ) <sub>$n$</sub>  – FID], recycle delay = 1.0 s [to allow  $T_1$  relaxation];  $\tau$  = ‘variable’ [to permit broad signal attenuation ( $T_2$  filter) and refocusing of spin-coupled multiplets];  $n$  = ‘variable’ [for a fixed loop cycle].

For application of the CPMGPR1D pulse sequence, arrays of  $\tau$  and  $n$  values were studied. With  $n$  fixed to 128 cycles, a wide range of  $\tau$  values (100, 300, 500, 670, and 800  $\mu$ s; 1.0, 1.3, 1.5, 1.7, 2.0, 2.5, 3.0, and 6.0 ms) was tested. The value of  $n$  was also varied (5, 20, 64, 128, 256 cycles) with  $\tau$  fixed to 500  $\mu$ s or 1.0 ms.

Typically, <sup>1</sup>H NMR data were collected with 128 scans and 65,536 data points using a 6.7  $\mu$ s pulse width (90° pulse angle) and a 3.27 s acquisition time with the same receiver gain. The total experiment time was about 30 minutes. Spectra of one sample were collected at various periods of time for 24 h and no obvious alterations were observed in the <sup>1</sup>H CPMG HR-MAS NMR spectra of S180 cells in a period of approximately 4 h.

Prior to Fourier transformation (FT), FIDs were zero-filled and an exponential weighing factor corresponding to 0.3 Hz line broadening applied. The acquired NMR spectra were

phase-corrected and referenced using TMSP-d<sub>4</sub> as internal reference. For metabolite assignment, gTOCSY and gCOSY experiments were carried out using default parameters.

## Results

### Comparison of pulse sequences

Figure 1 shows the <sup>1</sup>H HR-MAS NMR spectra of a fresh sample using: *i*) ZGPR; *ii*) ZGCPPR; *iii*) NOESY1DPR and *iv*) CPMGPR1D. Qualitative analysis revealed no evident changes in metabolite signals caused by the water suppression.

The pulse sequences differed significantly in water signal attenuation. The quality of residual water suppression

was good for ZGCPPR (Figure 1B) and CPMGPR1D (Figure 1D). However, both sequences caused distortions in the baseline around the water signal. It is clear that the suppression band for ZGPR (Figure 1A) was the broadest, although signal intensity was lower than NOESY1DPR (Figure 1C).

Furthermore, detailed examination of ZGPR, ZGCPPR and NOESY1DPR spectra revealed broad metabolite signals, as shown in Figure 2. With a T2 filter in the CPMGPR1D acquisition sequence (Figure 2D), narrower lines were obtained, and a better visualization of S180 metabolites achieved.

Therefore, a more detailed study of T2 filtering was undertaken to optimize the suppression of macromolecule signals, especially those from proteins. Firstly, an array of

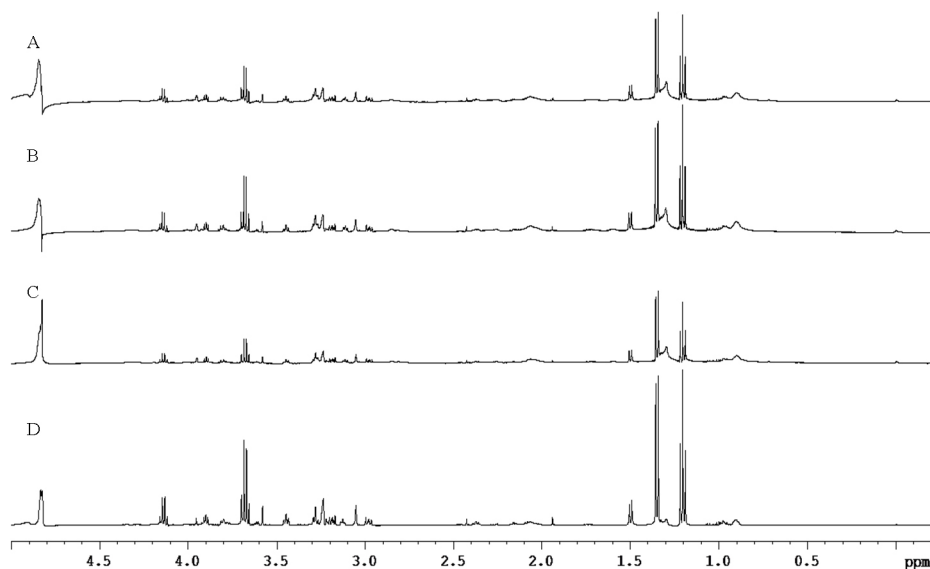


**Figure 1** Expansion/Detail of H<sub>2</sub>O signal suppression from <sup>1</sup>H HR-MAS NMR spectra (D<sub>2</sub>O, 500 MHz) of S180 cells using A) ZGPR, B) ZGCPPR, C) NOESY1DPR and D) CPMGPR1D pulse sequences.

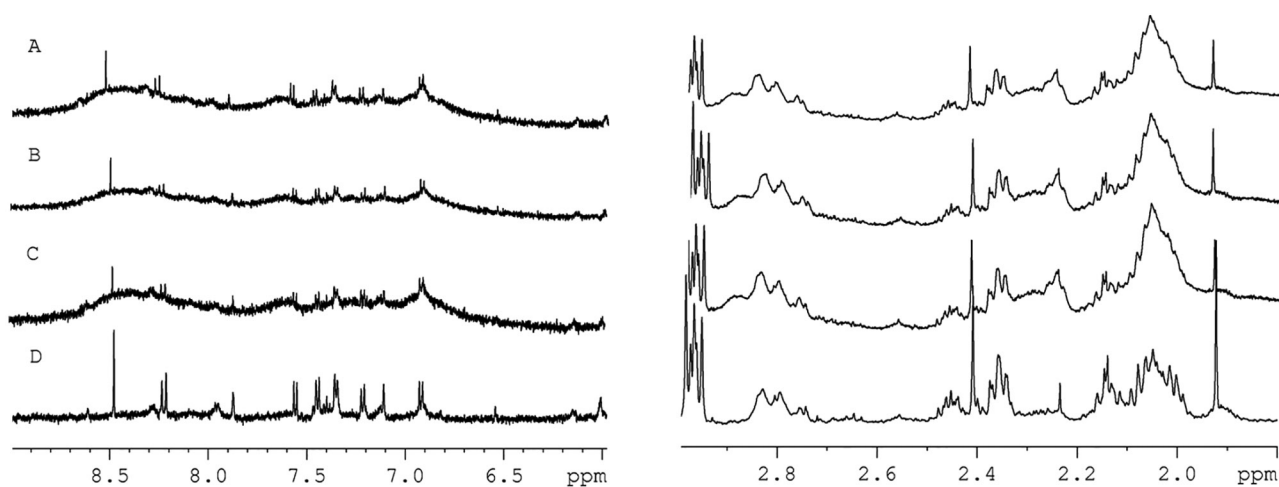


**Figure 2.** Expansion/detail of S180 cell <sup>1</sup>H HR-MAS NMR spectra (D<sub>2</sub>O, 500 MHz) comparing the resolution obtained using A) ZGPR, B) ZGCPPR, C) NOESY1DPR and D) CPMGPR1D pulse sequences.

the delay ( $\tau$ ) between 180° pulses was tested (100, 300, 500, 670 and 800  $\mu$ s; 1.0, 1.3, 1.5, 1.7, 2.0, 2.5, 3.0 and 6.0 ms) with  $n$  fixed at 128 cycles.

Seven different spectra are shown to the same scale in Figure 3, with echo times selected to show the most prominent differences. As seen in Figures 3A to 3C, extremely large values of  $\tau$  (greater than 2.0 ms) led to loss of the signal of interest or revealed signals with unsatisfactory intensities. On the other hand, very small values of  $\tau$  (500 and 100  $\mu$ s) did not suppress broad signals (Figures 3F and 3G).

Thus, intermediate  $\tau$  values were optimal for acquisition of <sup>1</sup>H HR-MAS NMR spectra, as shown in Figures 3D and 3E. The signals of small molecules remained apparent; likewise, the broad signals of macromolecules were filtered at both  $\tau$  values (1.5 and 1.0 ms). The signal-to-noise ratio was better at  $\tau = 1.0$  ms, mainly in the aromatic region; hence, this value was selected.

The number of cycles ( $n = 256, 128, 64, 20, 5$ ) was also optimized. When smaller values of  $n$  were used,

macromolecules gave broad and overlapping signals (Figures 4A, 4B and 4C), hiding potentially important signals from metabolites. As shown in Figure 4D, at  $n = 128$  the signal-to-noise ratio was increased; furthermore, no broad signals from macromolecules were observed. By contrast, a larger value of  $n$  (Figure 4E) reduced spectral sensitivity.

The optimal experimental conditions for the CPMGPR1D pulse sequence were thus found to be  $\tau = 1$  ms and  $n = 128$ , giving a total spin-spin relaxation delay ( $2n\tau$ ) of 256 ms. This filtered broad signals without reducing the signal-to-noise ratio.

#### Assignment of S180 cell metabolites

Comparison of high-resolution CPMG spectra with literature data<sup>18-24</sup> and two dimensional proton-proton spectroscopy (gTOCSY and gCOSY – data not shown) between  $\delta$  0.5 and 8.5 allowed the identification and signal assignment of twenty different metabolites (Table 1).

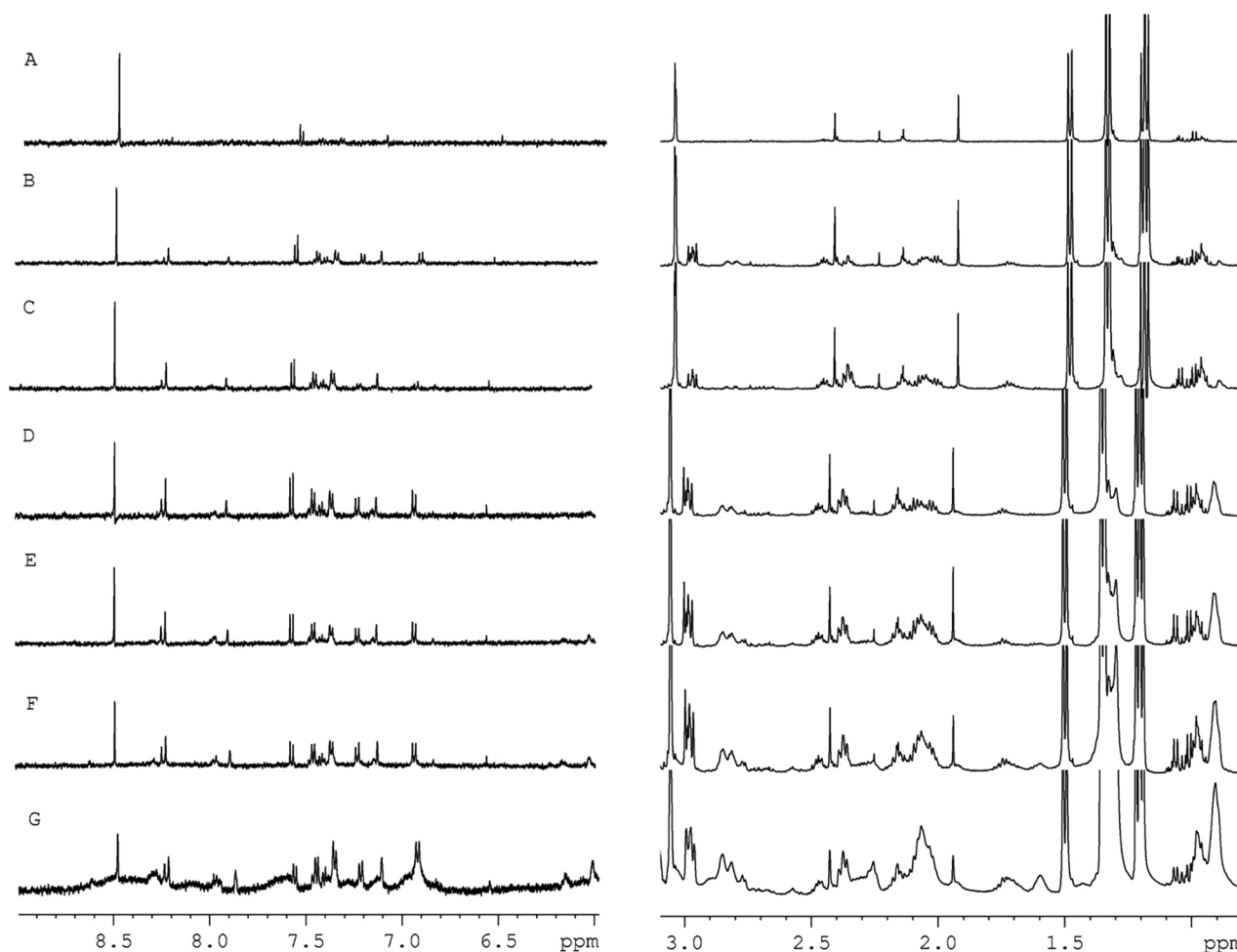


**Figure 3.** Expansion/detail of S180 cell <sup>1</sup>H HR-MAS NMR spectra (D<sub>2</sub>O, 500 MHz) using a CPMGPR1D pulse sequence with different values of  $\tau$ : (A) 6.0 ms, (B) 2.5 ms, (C) 2.0 ms, (D) 1.5 ms, (E) 1.0 ms, (F) 500  $\mu$ s and (G) 100  $\mu$ s. The  $\tau$  values shown were selected to reveal the most prominent differences in the spectra.

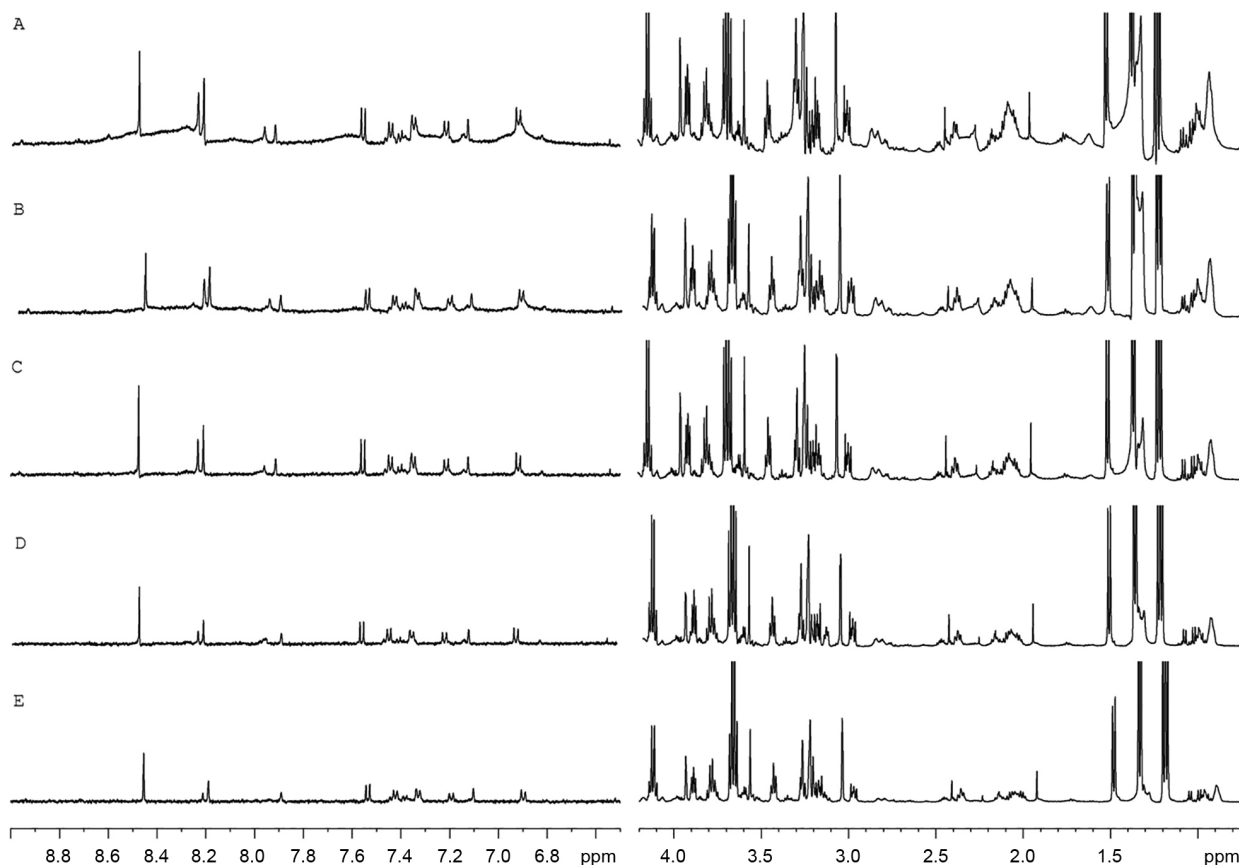


**Figure 4.** Expansion/detail of S180 cell  $^1\text{H}$  HR-MAS NMR spectra ( $\text{D}_2\text{O}$ , 500 MHz) using a CPMGPR1D pulse sequence with different numbers of cycles: (A) 5, (B) 20, (C) 64, (D) 128 and (E) 256 ( $\tau$  fixed to 1.0 ms). The  $n$  values were selected to reveal the most prominent differences in the spectra.

Compounds, chemical shifts and assignments are shown in Figure 5 and Table 1.

## Discussion

As typically found in cells and tissue samples, water gave a stronger signal in S180 cells than metabolites. This resonance must be suppressed to acquire high-quality NMR data, avoiding signal overlap and dynamic range problems. It is well known that NMR is a technique of low sensitivity. Reducing the water signal allows acquisition with the largest possible receiver gain. As a result, metabolites at low concentrations that may be important for profile discrimination can be detected. In addition, adequate water suppression allows the acquisition of reproducible spectra, which facilitates the use of statistical and quantitative techniques for metabolomic studies.

Several types of pulse sequence are available for suppression of water signals. In particular, Chen and co-authors<sup>13,14</sup> describe pulse sequences for water suppression in HR-MAS experiments on cells and tissues. They show that the strong coupling of membrane lipids to water inherent to HR-MAS NMR makes water suppression

difficult. Thus, it is necessary to develop methods enabling efficient water suppression for intact cells and tissue samples without also suppressing metabolite signals.<sup>13,14</sup> In this work, we tested four pulse sequences for this purpose. Although all the tested pre-saturation and composite pulse sequences successfully removed the water signal, the ZGCPPR and CPMGPR1D sequences gave the best results (Figure 1). Under optimal conditions, the residual water signal was narrowed and suppressed without perturbing other signals or the baseline.

Another factor taken into consideration was the need for a clear spectrum with good visualization of metabolite resonances because this can be used to characterize the cell's metabolite profile. Because macromolecules are inevitably found in biological matrices, the spectral resolution and analysis of signals may be dramatically affected by their broad resonances. Thus, the choice of pulse sequence to optimize spectral resolution is very important.

Although the water signal was narrowed by the chosen acquisition sequences, the removal of signals from large molecules with short transverse relaxation times improved the resolution of the peaks from significant metabolites,

**Table 1.** Chemical shift assignments for metabolites from <sup>1</sup>H HR-MAS NMR spectra of S180 cells (D<sub>2</sub>O, 500 MHz)

Assigned number	Metabolite		Multiplicity	J / Hz	δ / ppm
1	Fatty acids	-CH <sub>3</sub>	m	c	0.90
		-(CH <sub>2</sub> ) <sub>n</sub>	m	c	1.30
		-CH <sub>2</sub> -CH <sub>2</sub> -CO-	m	c	1.59
		-CH=CH-CH <sub>2</sub> -CH <sub>2</sub>	m	c	2.04
		-CH <sub>2</sub> -CH <sub>2</sub> -CO-	m	c	2.26
		-CH=CH-CH <sub>2</sub> -CH=CH-	m	c	5.33
2	Isoleucine	δCH <sub>3</sub>	t	7.45	0.95
		γCH <sub>3</sub>	d	6.99	1.02
3	Leucine	δCH <sub>3</sub>	t	5.85	0.97
4	Valine	γCH <sub>3</sub>	d	7.00	1.00
		γ'CH <sub>3</sub>	d	7.00	1.05
5	Ethanol	βCH <sub>3</sub>	t	7.12	1.19
		αCH <sub>3</sub>	q	7.12	3.66
6	Lactate	βCH <sub>3</sub>	d	6.95	1.34
		αCH	q	6.95	4.13
7	Alanine	βCH <sub>3</sub>	d	7.21	1.49
		αCH	q	7.21	3.78
8	Acetate	CH <sub>3</sub>	s	-	1.93
9	Glutamate	βCH <sub>2</sub>	m	c	2.09
		γCH <sub>2</sub>	m	c	2.36
10	Succinate	α,βCH <sub>2</sub>	s	-	2.42
11	Creatine	CH <sub>3</sub>	s	-	3.05
		CH <sub>2</sub>	s	-	3.94
12	Choline	N(CH <sub>3</sub> ) <sub>3</sub>	s	-	3.21
13	Phosphocholine	N(CH <sub>3</sub> ) <sub>3</sub>	s	-	3.23
14	Glycerophosphocholine	N(CH <sub>3</sub> ) <sub>3</sub>	s	-	3.24
15	Taurine	N-CH <sub>2</sub>	t	6.66	3.28
		S-CH <sub>2</sub>	t	6.66	3.44
16	Glycine	βCH <sub>2</sub>	s	-	3.58
17	Uracil	C6H	d	7.65	5.81
		C5H	d	7.65	7.54
18	Tyrosine	C3H, 5H	d	8.54	6.90
		C2H, 6H	d	8.54	7.20
19	Histidine	C2H	s	-	8.20
20	Inosine	C2H	s	-	8.22
		C8	s	-	8.47

Chemical shifts are referenced relative to TMSP-d<sub>4</sub>. Abbreviations – s: singlet, d: doublet, t: triplet, q: quartet, m: multiplet, c: coupling constant not determined. Compound numbers correspond to those in Figure 5.

especially those between 2.0 to 3.0 ppm and 6.5 to 8.5 ppm (Figure 2). In fact, application of a T2 filter in the CPMGPR1D sequence facilitated the evaluation of cell metabolic profile.

Given that CPMGPR1D showed better-resolved signals because of its T2 filter, the optimization of τ and n values permitted improvement of spectral quality. To our knowledge, the optimization of 2τn values of the T2 filter in CPMG pulse sequence applied to cell samples has not been reported previously.

Although small molecules have large transverse relaxation times, very large values of τ (greater than 2.0 ms, Figures 3A to 3C) permitted transverse relaxation for both types of molecule (small and macro-). Thus, large values of τ should be avoided.

In contrast, when τ values were lower than T2 for macromolecules, the broad signals overlapped the signals of low molecular weight metabolites. Therefore, intermediate values of τ (Figures 3D and 3E) ensured that macromolecules were properly filtered without the disappearance of small molecules. When the τ value was 1.0 ms (Figure 3E), the signal/noise ratio was better than 1.5 ms (noise was slightly superior). We therefore suggest that a value of 1.0 ms should be used in future studies with S180 cells.

For optimization of the number of cycle loops (n), even when the τ value was optimal, smaller values of n masked metabolite signals because the macromolecules did not relax completely by T2, appearing in the spectra as broad resonances (Figures 4A, B and C).

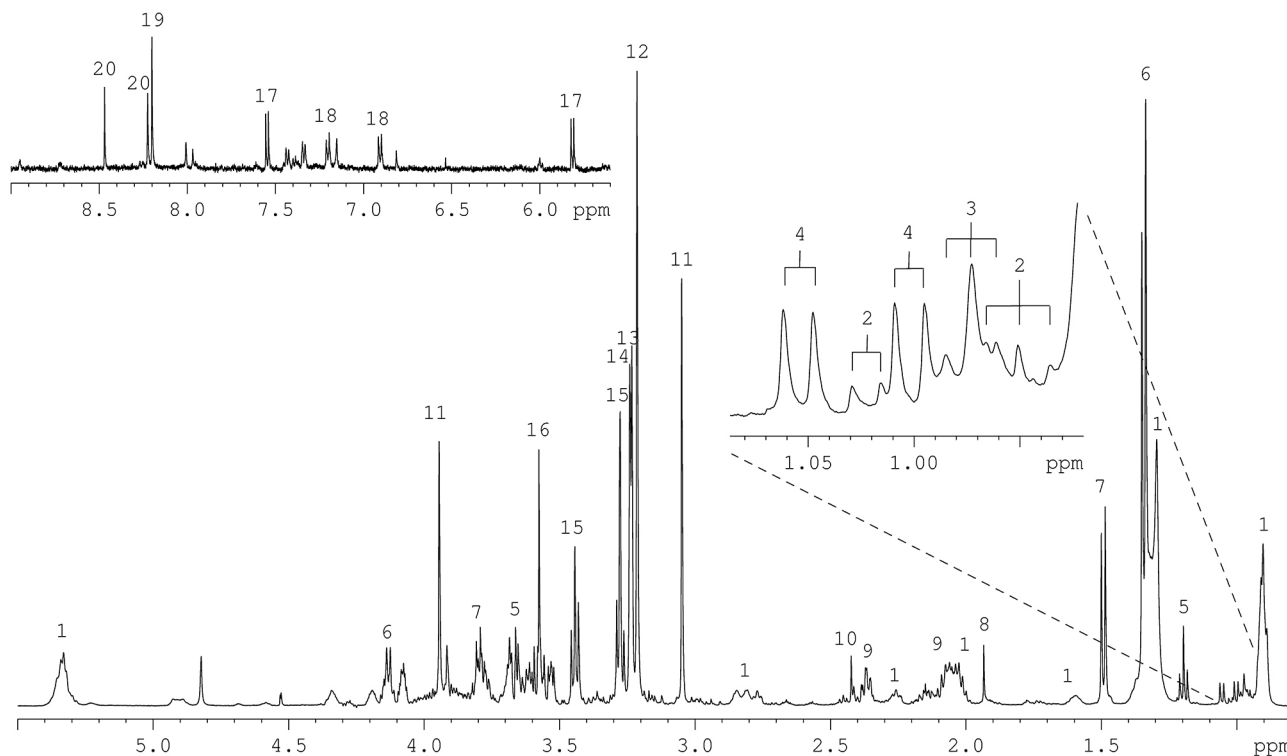


**Figure 5.**  $^1\text{H}$  HR-MAS NMR spectrum of S180 cells ( $\text{D}_2\text{O}$ , 500 MHz) with spectral assignments of metabolites numbered (see Table 1 for numbering).

In Figure 4D, at  $n = 128$  the signal-to-noise ratio increased and no interfering broad signals from macromolecules were observed. This  $n$  value led to an enhancement in resolution and sensitivity; the signals that were reduced by this method had low intensity and appeared as an elevation of the baseline overlapping the signals of small molecules.

A larger value of  $n$  (Figure 4E) decreased spectral sensitivity because small molecules were also T2-filtered. This value also increased total analysis time.

For these reasons, in NMR analyses of cells and tissues using the CPMG pulse sequence,  $\tau$  values should be kept low and the number of cycles ( $n$ ) should be increased appropriately to increase total T2 relaxation delay.

Moreover, it is important to highlight that  $\tau$  and  $n$  parameters are directly related, and therefore each value of  $\tau$  will present an optimal value of  $n$ . Then, for  $\tau = 1$  ms,  $n = 128$  cycles is the optimal experimental conditions for the CPMGPR1D pulse sequence.

A complete assignment of metabolite profile was obtained, which should be of value in future work with S180 cells. Most of these metabolites are composed of amino acids and membrane components such as lipids and choline derivatives. This systematic analysis is appealing because it has been shown in cellular models that these resonances may act as cell proliferation markers.<sup>25</sup> Thus, they may provide additional information for discrimination of

tumor types. For instance, it has been reported that choline derivatives are associated with accelerated cell proliferation; as precursors of phospholipid membranes, they can be used as cell proliferation biomarkers.<sup>25-27</sup>

## Conclusion

This work has addressed a number of important problems regarding the practical application of HR-MAS NMR spectroscopy to the study of S180 cells. The optimal experimental conditions for the CPMGPR1D pulse sequence were found to be  $\tau = 1$  ms and  $n = 128$  cycles, giving a total spin-spin relaxation delay ( $2n\tau$ ) of 256 ms. Sensitivity and resolution, and consequently the quality of spectra obtained from S180 cells, were improved by the optimized pulse sequence.

Using the optimized HR-MAS NMR experiment, the assignment of twenty different metabolites was possible. This information may be a guide for metabolomic research using the HR-MAS NMR technique in S180 cells because it provides the chemical profile of these cells.

## Acknowledgements

We thank CNPq (PRODOC 52001016035P5), CAPES (Casadinho620014/2008-3) and MCT/FINEP/CT-INFRA - PROINFRA 01/2004 for their financial support.

## References

1. Sitter, B.; Bathen, T. F.; Tessem, M. B.; Gribbestad, I. S.; *Prog. Nucl. Magn. Reson. Spec.* **2009**, *54*, 239.
2. Valverde-Saubí, D.; Candiota, A. P.; Molins, M. A.; Feliz, M.; Godino, O.; Dávila, M.; Acebes, J. J.; Arús, C.; *Magn. Reson. Mater. Phys. Biol. Med.* **2010**, *23*, 203.
3. Andronesi, O. C.; Blekas, K. D.; Mintzopoulos, D.; Astrakas, L.; Black, P. M.; Tzika, A. A.; *Int. J. Oncol.* **2008**, *33*, 1017.
4. Sitter, B.; Bathen, T. F.; Singstad, T. E.; Fjøsne, H. E.; Lundgren, S.; Halgunset, J.; Gribbestad, I. S.; *NMR Biomed.* **2010**, *23*, 4424.
5. Chan, E. C.; Koh, P. K.; Mal, M.; Cheah, P. Y.; Eu, K. W.; Backshall, A.; Cavill, R.; Nicholson, J. K.; Keun, H. C.; *J. Proteome Res.* **2009**, *8*, 352.
6. Rocha, C. M.; Barros, A. S.; Gil, A. M.; Goodfellow, B. J.; Humpfer, E.; Spraul, M.; Carreira, I. M.; Melo, J. B.; Bernardo, J.; Gomes, A.; Sousa, V.; Carvalho, L.; Duarte, I. F.; *J. Proteome Res.* **2010**, *9*, 319.
7. Mirbahai, L.; Wilson, M.; Shaw, C. S.; McConville, C.; Malcomson, R. D.; Griffin, J. L.; Kauppinen, R. A.; Peet, A. C.; *Int. J. Biochem. Cell Biol.* **2011**, *43*, 990.
8. Chiaradonna, F.; Moresco, R. M.; Airoidi, C.; Gaglio, D.; Palorini, R.; Nicotra, F.; Messa, C.; Alberghina, L.; *Biotechnol. Adv.* **2012**, *30*, 30.
9. Backshall, A.; Alferez, D.; Teichert, F.; Wilson, I. D.; Wilkinson, R. W.; Goodlad, R. A.; Keun, H. C.; *J. Proteome Res.* **2009**, *8*, 1423.
10. Decelle, E. A.; Cheng, L. L.; *NMR Biomed.* **2014**, *27*, 90.
11. Duarte, I. F.; Ladeirinha, A. F.; Lamego, I.; Gil, A. M.; Carvalho, L.; Carreira, I. M.; Melo, J. B.; *Mol. Pharmaceutics* **2013**, *10*, 4242.
12. Aranbar, N.; Ott, K.; Roongta, V.; Mueller, L.; *Anal. Biochem.* **2006**, *355*, 62.
13. Chen, J. H.; Sambol, E. B.; Kennealey, P. T.; Connor, R. B. O.; Carolis, P. L.; Cory, D. G.; Singer, D.; *J. Magn. Reson.* **2004**, *171*, 143.
14. Chen, J. H.; Sambol, E. B.; DeCarolis, P.; Connor, R. B. O.; Geha, R. C.; Wu, Y. V.; Singer, S.; *Magn. Reson. Med.* **2006**, *55*, 1246.
15. Wang, X. B.; Liu, Q. H.; Wang, P.; Tang, W.; Hao Q.; *Ultrasonics* **2008**, *48*, 135.
16. Chen, Y.; Chen, J.; Xu, S.; Wang, Y.; Li, X.; Cai, B.; Fan, N.; *Bioorg. Med. Chem. Lett.* **2012**, *22*, 2717.
17. Xue, R.; Cao, Y.; Han, N.; Lin, X.; Liu, Z.; Yin J.; *J. Ethnopharmacol.* **2011**, *137*, 1156.
18. Moestue, S. A.; Borgan, E.; Huuse, E. M.; Lindholm, E. M.; Sitter, B.; Børresen-Dale, A. L.; Engebraaten, O.; Maeldandsmo, G. M.; Gribbestad, I. S.; *BMC Cancer* **2010**, *10*, 433.
19. Sitter, B.; Sonnewald, U.; Spraul, M.; Fjøsne, H. E.; Gribbestad, I. S.; *NMR Biomed.* **2002**, *15*, 327.
20. Martínez-Bisbal, M. C.; Esteve, V.; Martínez-Granados, B.; Celda, B.; *J. Biomed. Biotech.* **2011**, ID 763684.
21. Borgan, E.; Sitter, B.; Lingjaerde, O. C.; Johnsen, H.; Lundgren, S.; Bathen, T. F.; Sørli, T.; Børresen-Dale, A. L.; Gribbestad, I. S.; *BMC Cancer* **2010**, *10*, 628.
22. Teahan, O.; Bevan, C. L.; Waxman, J.; Keun, H. C.; *Int. J. Biochem. Cell Biol.* **2011**, *43*, 1002.
23. Bathen, T. F.; Jensen, L. R.; Sitter, B.; Fjøsne, H. E.; Halgunset, J.; Axelson, D. E.; Gribbestad, I. S.; Lundgren, S.; *Breast Cancer Res. Treat.* **2007**, *104*, 181.
24. Seierstad, T.; Roe, K.; Sitter, B.; Halgunset, J.; Flatmark, K.; Ree, A. H.; Olsen, D. R.; Gribbestad, I. S.; Bathen, T. F.; *Mol. Cancer* **2008**, *7*, 33.
25. Barba, I.; Cabañas, M. E.; Arús, C.; *Cancer Res.* **1999**, *59*, 1861.
26. Stenman, K.; Stattin, P.; Stenlund, H.; Riklund, K.; Gröbner, G.; Bergh, A.; *Biomarker Insights* **2011**, *6*, 39.
27. Glunde, K.; Jacobs, M. A.; Bhujwala, Z. M.; *Expert Rev. Mol. Diagn.* **2006**, *6*, 821.

Submitted: December 21, 2013

Published online: April 8, 2014